MODELING TRAFFIC JAMS IN INTRACELLULAR TRANSPORT IN AXONS

How can this model shed light on the mechanisms that can cause traffic jams in neurons?

Student: Urszula Maria Starowicz
Lecturer: Steinar Evje

Mutations in molecular motors can disrupt intracellular transport within axons, leading to traffic congestion. These blockages often cause axonal swelling, contributing to various neurodegenerative diseases. This project aims to investigate a model that describes the formation of traffic jams in axons during the molecular-motor-driven transport of intracellular organelles.

1. **Introduction**

   (i) Write a brief summary of the engineering problem to be explored (use illustration). Make it short and concise.

   Intracellular transport in axons is a critical process that ensures the delivery of essential biomolecules and organelles along the length of a neuron. This transport is facilitated by molecular motors moving along microtubules, carrying cargo bidirectionally between the cell body and synaptic terminals. Disruptions in this transport system are linked to neurodegenerative diseases such as Alzheimer's and Parkinson's.

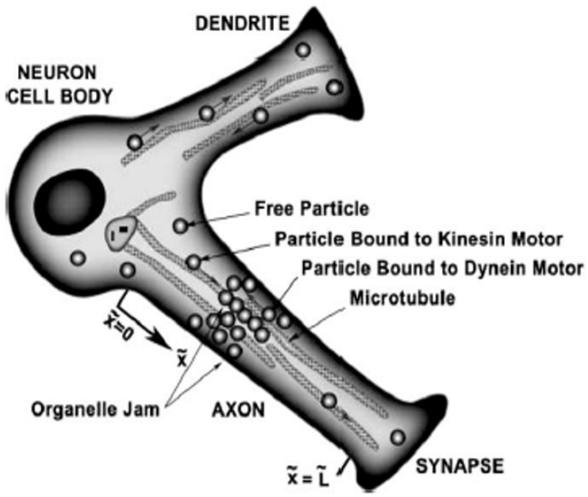

Figure 1: Schematic diagram of a neuron cell with a dendrite and axon.

   (ii) Present the mathematical model that can be used for that purpose with the different variables and parameters.

   The molecular-motor-assisted transport equations suggested in Smith and Simmons are given by:

$$\frac{\partial \tilde{n_0}}{\partial t} = D_0 \frac{\partial^2 \tilde{n_0}}{\partial x^2} - (\tilde{k}^+ + \tilde{k}^-)\tilde{n_0} + \tilde{k}_0 \tilde{n_0} + \tilde{k}^- \tilde{n} \quad (1)$$

$$\frac{\partial \tilde{n^+}}{\partial t} = \tilde{k}^+ \tilde{n_0} - \tilde{k}_0 \tilde{n^+} + \frac{\partial}{\partial x}(\tilde{v}^+ \tilde{n^+}) \quad (2)$$

$$\frac{\partial \tilde{n^-}}{\partial t} = \tilde{k} \tilde{n_0} - \tilde{k}_0 \tilde{n^-} - \frac{\partial}{\partial x}(\tilde{v} \tilde{n}) \quad (3)$$

where:

- D_0 is the diffusivity of a free particle.
- $\tilde{n_0}$ is the concentration of free particles.
- $\tilde{n^+}$ is the concentration of particles moving on microtubules in the positive direction (away from the cell body).
- $\tilde{n}$ is the concentration of particles moving on microtubules in the negative direction (toward the cell body).
- x is the linear coordinate along the axon.
- $\tilde{v}$ is the velocity of a particle moving on a microtubule toward the cell body (generated by dynein-family molecular motor).
- $\tilde{v}^+$ is the velocity of a particle moving on a microtubule away from the cell body (generated by kinesin-family molecular motor).
- $\tilde{k}^+$ and $\tilde{k}^-$ are the first-order rate constants for binding to microtubules for particles that move in the positive and negative directions, respectively.
- $\tilde{k}_0^+$ and $\tilde{k}_0^-$ are the first-order rate constants for detachment from microtubules for particles that move in the positive and negative directions, respectively.

These equations are solved subject to the following boundary conditions:

$$x = 0: \quad \tilde{n_0} = eN_0, \quad \tilde{n^+} = r_0 eN_0 \quad (4)$$

$$x = L: \quad \tilde{n_0} = eN_L, \quad \tilde{n} = r_L eN_L$$

(iii) Describe briefly the purpose of each transport equation and also the specific role played by the different terms.

Equation 1: This equation models the evolution of the free particle concentration ($\tilde{n_0}$) along the axon. The terms account for diffusion, binding of particles to microtubules, and detachment from microtubules.

Equation 2: This equation describes the concentration of particles moving in the positive direction ($\tilde{n^+}$). It includes binding to microtubules, detachment from them, and the transport of particles along the microtubules at a positive velocity.

Equation 3: This equation represents the concentration of particles moving in the negative direction ($\tilde{n}$). It includes binding to microtubules, detachment, and the transport of particles along the microtubules at a negative velocity.

(iv) Try to bring forth a few relevant research questions that could be of interest to explore based on the set-up shown in the schematic figure 1.

i. How do variations in the binding and detachment rates of molecular motors affect the formation of traffic jams in axons?

ii. What is the role of the diffusivity of free particles (D_0) in the accumulation and dispersal of cargo within the axon?

iii. How does the interaction between particles moving in opposite directions (e.g., kinesin and dynein-driven transport) influence the development of axonal traffic jams?

iv. Does diffusion or change in the speed of traffic cause more damage to the flow of the transportation?

(v) Explain why you will need to know how to deal with a generic advection equation of the form:

$$u_t + a(x,t)u_x = q(x,t,u) \tag{1}$$

Understanding how to deal with a generic advection equation of the form given above is essential because this type of equation describes the transport of a quantity (e.g., particle concentration, temperature, or chemical concentration) through a medium. In the context of the molecular motor-assisted transport model, the advection equation represents the movement of particles along microtubules. The key reasons for understanding it are:

Representation of Transport Dynamics:
The equation models the transport of particles as they move in space and time, with the advection term $a(x,t)u_x$ capturing the effect of velocity or motor-driven transport. Solving this equation helps in understanding how particles move and accumulate in different regions over time.

Time and Space Dependencies:
The term $a(x,t)$ allows the advection velocity to vary with position and time, which is critical in biological systems where transport rates may change due to local environmental factors (e.g., motor proteins switching or varying transport speeds along the axon). This helps capture spatially dependent transport behaviors.

Source and Sink Terms:
The term $q(x,t,u)$ represents external influences such as production or degradation, which is necessary to model processes like particle attachment or detachment from microtubules in the presence of source/sink terms.

Boundary and Initial Conditions:
Solving this equation requires handling boundary conditions and initial distributions, which helps determine how the concentration of particles evolves in space and time, accurately reflecting experimental observations.

Numerical Methods:
The equation is often solved numerically, especially when dealing with complex, spatially-varying transport. This requires methods such as finite difference or finite element methods. Understanding how to work with such equations enables effective application of these techniques to obtain solutions that match real-world phenomena.

In summary, mastering the advection equation allows for accurate prediction and analysis of transport dynamics in systems such as the microtubule transport model.

Summary This task explores the intracellular transport process in axons, focusing on the role of molecular motors that move cargo bidirectionally on microtubules. The disruption of this transport system is associated with neurodegenerative diseases such as Alzheimer's and Parkinson's. The mathematical model consists of a set of partial differential equations that describe the concentration of free particles and their movement along microtubules in both directions. These equations include terms for diffusion, binding, and detachment processes. Research questions arise regarding the impact of varying molecular motor rates, the diffusivity of free particles, and the interaction between particles moving in opposite directions. The advection equation, which governs particle transport, is essential for understanding the accumulation and dispersal of cargo. Solving this equation provides insight into how transport disruptions might lead to axonal traffic jams and related diseases. Understanding the dynamics of the advection equation is crucial for analyzing transport systems in biological contexts.

2. Theory and methods

Initial data sheared by all three of the problems are:

$$u_0(x) = \begin{cases} 1, & 0.8 \leq x \leq 1.2, \\ 0, & \text{otherwise.} \end{cases} \tag{2}$$

The computational domain has a length of $L_{\text{dom}} = 2.0$ and is discretized using grid cells $M = 500$, resulting in a grid spacing of:

$$\Delta x = \frac{L_{\text{dom}}}{M} = 0.004 \tag{3}$$

To ensure a stable discretization. The total number of time steps required to reach $T = 0.5$ is:

$$N_{\text{Time}} = \frac{T}{\Delta t}. \tag{4}$$

(a) Linear problem I

$$u_t + a u_x = 0, \quad a > 0 \tag{5}$$

with the initial condition:

$$u(x, t = 0) = u_0(x), \quad x \in [0, 2] \tag{6}$$

The time step is chosen as:

$$\Delta t = \Delta x. \tag{7}$$

The number of time steps required to reach $T = 0.5$ is:

$$N_{\text{Time}} = \frac{T}{\Delta t} = 125. \tag{8}$$

The Courant–Friedrichs–Lewy (CFL) condition is checked to ensure numerical stability:

$$\lambda_1 = \frac{\Delta t}{\Delta x}, \quad \text{and it must satisfy} \quad a\lambda_1 \leq 1. \tag{9}$$

The result of the simulation:

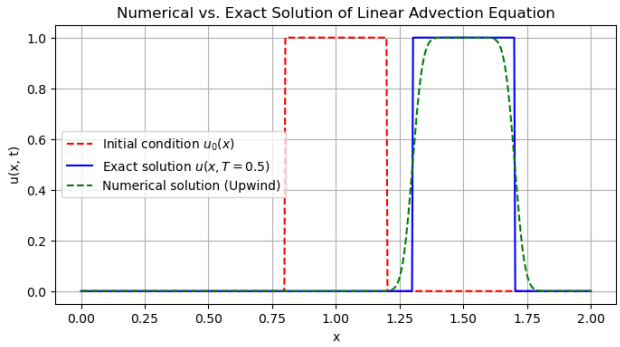

Figure 2: Solution for simulation of the linear problem I.

(b) Linear problem II

$$u_t + xu_x = 0, \quad x \in [0, 2] \tag{10}$$

with the initial condition:

$$u(x, t = 0) = u_0(x). \tag{11}$$

The time step is chosen as:

$$\Delta t = \frac{\Delta x}{L_{\text{dom}} T}, \tag{12}$$

The CFL condition is given by:

$$\lambda_1 = \frac{\Delta t}{\Delta x}. \tag{13}$$

To obtain the exact solution, we use the method of characteristics. The characteristic equations are given by:

$$\frac{dx}{dt} = x. \tag{14}$$

To solve this we separate the variables:

$$\frac{dx}{x} = dt. \tag{15}$$

Next, we integrate both sides:

$$\int \frac{dx}{x} = \int dt. \tag{16}$$

Evaluating the integrals:

$$\ln |x| = t + C, \tag{17}$$

where C is the constant of integration. Exponentiating both sides:

$$x = e^{t+C}. \tag{18}$$

Using the property $e^{t+C} = e^C e^t$, we define $e^C = x_0$ (a new constant), giving:
Solving this gives the characteristic curves:

$$x(t) = x_0 e^t, \tag{19}$$

where x_0 is the initial position. Along these characteristics, $u(x,t)$ remains constant, implying:

$$u(x,t) = u_0(x_0). \tag{20}$$

Substituting $x_0 = xe^{-t}$, we obtain the exact solution:

$$u(x,t) = u_0(xe^{-t}). \tag{21}$$

The results for this simulation:

i. Adjusted $\Delta t = 0.002$ s.
ii. Number of time steps is 250.
iii. Numerical solution error is about 0.128.

Result of the simulation:

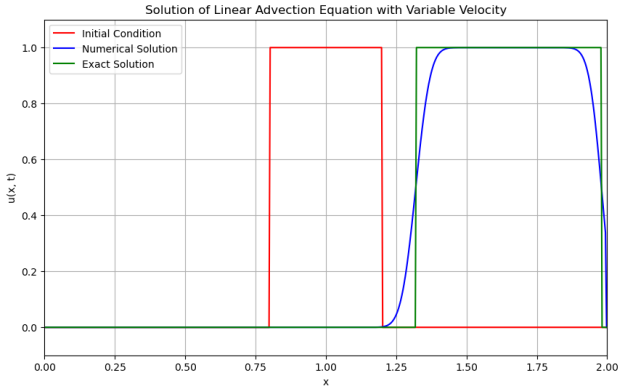

Figure 3: Solution for simulation of the linear problem II.

(c) Linear problem III

Let's consider the following problem:

$$u_t + u_x = x, \quad x \in [0, 2] \tag{22}$$

with the initial condition:

$$u(x, t = 0) = u_0(x). \tag{23}$$

Characteristic Equations

The characteristic equations are obtained by rewriting the PDE in the form:

$$\frac{dt}{1} = \frac{dx}{1} = \frac{du}{x}. \tag{24}$$

From the first equation, we get the characteristic curves:

$$x - t = \text{constant} = x_0. \tag{25}$$

Thus, along a characteristic curve:

$$x = x_0 + t. \tag{26}$$

Solving for u

From the third equation:

$$\frac{du}{dt} = x. \tag{27}$$

Substituting $x = x_0 + t$, we obtain:

$$\frac{du}{dt} = x_0 + t. \tag{28}$$

Integrating both sides with respect to t:

$$u = x_0 t + \frac{t^2}{2} + C. \tag{29}$$

Using $x_0 = x - t$, we rewrite:

$$u = (x - t)t + \frac{t^2}{2} + C. \tag{30}$$

Applying the Initial Condition

From the initial condition $u(x, 0) = u_0(x)$, we set $t = 0$, giving:

$$C = u_0(x - t). \tag{31}$$

Thus, the final solution is:

$$u(x, t) = u_0(x - t) + xt - \frac{1}{2}t^2. \tag{32}$$

From the lecture notes (*Notes-1ef*), the solution is given by:

$$u(x, t) = u_0(x - t) + xt - \frac{1}{2}t^2. \tag{33}$$

The time step is chosen to satisfy the CFL condition:

$$\Delta t = \frac{\Delta x}{L_{\text{dom}} T}. \tag{34}$$

The Courant number is given by:

$$\lambda_1 = \frac{\Delta t}{\Delta x}. \tag{35}$$

The result of the simulation:

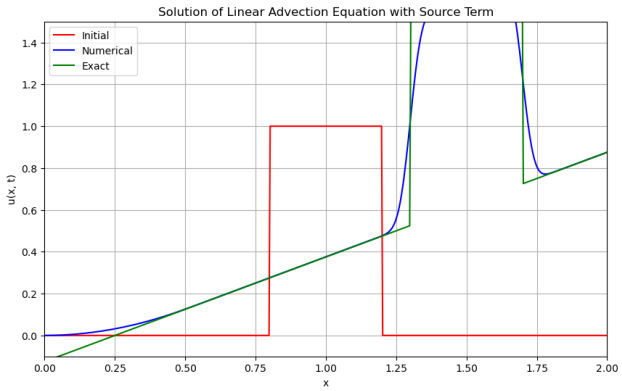

Figure 4: Solution for simulation of the linear problem III.

Summary This task involved solving three different linear partial differential equations (PDEs) using numerical methods. The shared initial condition for all problems was a piecewise function, where $u_0(x) = 1$ for $0.8 \leq x \leq 1.2$ and zero otherwise. The computational domain spanned $[0, 2]$ with $M = 500$ grid cells and a spatial resolution of $\Delta x = 0.004$. The time step was chosen based on stability conditions, leading to different values for each problem. The first problem considered the linear advection equation with constant velocity $u_t + au_x = 0$, where the time step was set to $\Delta t = \Delta x$, resulting in 125 time steps, with stability ensured by the CFL condition. The second problem involved a variable velocity $u_t + xu_x = 0$, where the exact solution was given by $u(x, t) = u_0(xe^{-T})$, the adjusted time step was $\Delta t = 0.002$ s, and the numerical solution error was approximately 0.128. The third problem introduced a source term in the equation $u_t + u_x = x$, with an analytical solution derived from lecture notes as $u(x, t) = u_0(x - t) + xt - \frac{1}{2}t^2$. The numerical results for each problem were analyzed and compared to the exact solutions.

3. **Investigations of traffic jams in intracellular transport in axons**

   a) Converting dimensional model into dimensionless model.

   The given mathematical model for intracellular transport in an axon is:

$$n_t = D_0 n_{xx} - (1 + k_-)n + k_p n^+ + k_n n^-, \quad x \in [0, L] \tag{36}$$

$$(n^+)_t + V_+(n^+)_x = n^- - k_p n^+ \tag{37}$$

$$(n^-)_t + V_-(n^-)_x = k_- n^- - k_n n^-. \tag{38}$$

   Introducing Dimensionless Variables

   To non-dimensionalize the equations, we introduce the following transformations:

$$\hat{x} = \frac{xk_+}{V_{+,0}}, \quad \hat{t} = tk_+, \quad \hat{D}_0 = \frac{D_0 k_+}{V_{+,0}^2}, \tag{39}$$

$$\hat{n} = \frac{nV_{+,0}^3}{k_+^3}, \quad \hat{n}^{\pm} = \frac{n^{\pm}V_{+,0}^3}{k_+^3}, \tag{40}$$

$$\hat{k}_- = \frac{k_-}{k_+}, \quad \hat{k}_p = \frac{k_p}{k_+}, \quad \hat{k}_n = \frac{k_n}{k_+}, \tag{41}$$

$$\hat{V}_- = \frac{V_-}{V_{+,0}}. \tag{42}$$

These transformations ensure that all variables are dimensionless, removing any units from the equations.

Transforming the Time and Space Derivatives

Applying the transformations:

$$\hat{x} = \frac{xk_+}{V_{+,0}}, \quad \hat{t} = tk_+$$

we compute the derivatives:

$$\frac{\partial}{\partial x} = \frac{\partial \hat{x}}{\partial x}\frac{\partial}{\partial \hat{x}} = \frac{k_+}{V_{+,0}}\frac{\partial}{\partial \hat{x}}, \tag{43}$$

$$\frac{\partial}{\partial t} = \frac{\partial \hat{t}}{\partial t}\frac{\partial}{\partial \hat{t}} = k_+\frac{\partial}{\partial \hat{t}}. \tag{44}$$

Similarly, for the second derivative:

$$\frac{\partial^2}{\partial x^2} = \left(\frac{k_+}{V_{+,0}}\right)^2 \frac{\partial^2}{\partial \hat{x}^2}. \tag{45}$$

Transforming the Diffusion Term

Using the transformation for D_0:

$$D_0 n_{xx} = D_0 \left(\frac{k_+}{V_{+,0}}\right)^2 \hat{n}_{\hat{x}\hat{x}} = \frac{D_0 k_+}{V_{+,0}^2}\hat{n}_{\hat{x}\hat{x}}. \tag{46}$$

Thus, using $\hat{D}_0 = \frac{D_0 k_+}{V_{+,0}^2}$, we rewrite:

$$D_0 n_{xx} = \hat{D}_0 \hat{n}_{\hat{x}\hat{x}}. \tag{47}$$

Transforming the Advection Terms

For the transport terms:

$$V_+\frac{\partial n^+}{\partial x} = V_+\left(\frac{k_+}{V_{+,0}}\right)\frac{\partial \hat{n}^+}{\partial \hat{x}}, \tag{48}$$

$$V_-\frac{\partial n^-}{\partial x} = V_-\left(\frac{k_+}{V_{+,0}}\right)\frac{\partial \hat{n}^-}{\partial \hat{x}}. \tag{49}$$

Using $\hat{V}_- = \frac{V_-}{V_{+,0}}$, we write:

$$V_+ \frac{\partial n^+}{\partial x} = \frac{k_+}{V_{+,0}} V_{+,0} \frac{\partial \hat{n}^+}{\partial \hat{x}} = k_+ \frac{\partial \hat{n}^+}{\partial \hat{x}}, \tag{50}$$

$$V_- \frac{\partial n^-}{\partial x} = k_+ \hat{V}_- \frac{\partial \hat{n}^-}{\partial \hat{x}}. \tag{51}$$

Transforming the Source Terms

For the reaction terms:

$$k_- n = k_- \frac{k_+^3}{V_{+,0}^3} \hat{n} = k_+ \hat{k}_- \hat{n}, \tag{52}$$

$$k_p n^+ = k_p \frac{k_+^3}{V_{+,0}^3} \hat{n}^+ = k_+ \hat{k}_p \hat{n}^+, \tag{53}$$

$$k_n n^- = k_n \frac{k_+^3}{V_{+,0}^3} \hat{n}^- = k_+ \hat{k}_n \hat{n}^-. \tag{54}$$

Substituting into the Original Equations

Dividing each equation by k_+ and rewriting in dimensionless form (dropping hats for simplicity):

$$n_t = D_0 n_{xx} - (1 + k^-) n + k_p n^+ + k_n n^-, \quad x \in [0, L] \tag{55}$$

$$(n^+)_t + (n^+)_x = n^- - k_p n^+ \tag{56}$$

$$(n^-)_t - (n^-)_x = k^- n^- - k^n n^-. \tag{57}$$

Next, the boundary conditions in dimensionless form are given by:

$$n|_{x=0} = N_0, \quad n^+|_{x=0} = N_0 \sigma_0, \tag{58}$$

$$n|_{x=L} = N_L, \quad n^-|_{x=L} = N_L \sigma_L. \tag{59}$$

These boundary conditions describe the concentrations of free particles and particles moving in positive and negative directions at the endpoints of the domain. At $x = 0$, the concentration of free particles is set to N_0, and the concentration of particles moving in the positive direction is given by $N_0\sigma_0$. Similarly, at $x = L$, the free particle concentration is N_L, and the concentration of particles moving in the negative direction is $N_L\sigma_L$. These conditions ensure that there is a controlled influx and efflux of particles at the domain boundaries, modeling realistic transport constraints in axons.

The initial conditions are:

$$n(x, t = 0) = N_0 + (N_L - N_0) \frac{x}{L}, \tag{60}$$

$$n^+(x, t = 0) = 0, \tag{61}$$

$$n^-(x, t = 0) = 0. \tag{62}$$

This completes the transformation of the model into its dimensionless form, making it more suitable for numerical analysis and comparison across different parameter settings.

b) Describe a discrete version of the traffic jam model (TJM).

To discretize the transport equations, we use a finite difference scheme. Let n_j^m represent the approximation of $n(x_j, t_m)$ on a uniform grid with spatial step Δx and temporal step Δt. The discrete versions of the equations are:

$$\frac{n_j^{m+1} - n_j^m}{\Delta t} = D_0 \frac{n_{j+1}^m - 2n_j^m + n_{j-1}^m}{(\Delta x)^2} - (1 + k_-)n_j^m + k_p n_j^{+,m} + k_n n_j^{-,m}, \tag{63}$$

$$\frac{n_j^{+,m+1} - n_j^{+,m}}{\Delta t} + V_+ \frac{n_{j+1}^{+,m} - n_j^{+,m}}{\Delta x} = n_j^{-,m} - k_p n_j^{+,m}, \tag{64}$$

$$\frac{n_j^{-,m+1} - n_j^{-,m}}{\Delta t} + V_- \frac{n_j^{-,m} - n_{j-1}^{-,m}}{\Delta x} = k_- n_j^{-,m} - k_n n_j^{-,m}. \tag{65}$$

The advection terms are discretized using an upwind scheme to maintain numerical stability. The diffusion term is approximated with a central difference scheme. The choice of time step Δt must satisfy the CFL condition for numerical stability:

$$\Delta t \leq \frac{\Delta x}{\max(|V_+|, |V_-|)}. \tag{66}$$

This discrete model allows for numerical simulation of traffic jams in intracellular transport.

c) Set the RHS of the model to zero.

To analyze the behavior of the simplified model, we implement a numerical scheme and generate plots to support the following observations:

Behavior of the Model

The model generates wave-like behavior for the advective equations governing n^+ and n^-, with transport occurring at constant velocity. The diffusion equation governing n results in a smooth spreading of concentration over time.

Simulation Period for Front Propagation

The fronts of n^+ and n^- propagate at constant speeds. A suitable simulation period can be estimated by considering the domain length L and characteristic velocities, ensuring the waves reach the domain boundaries.

Comparison with Exact Solutions

The exact solutions to the equations are:

$$n(x,t) = N_0 + (N_L - N_0)\frac{x}{L}, \tag{67}$$

$$n^+(x,t) = n^+(x - t), \tag{68}$$

$$n^-(x,t) = n^-(x + t). \tag{69}$$

These solutions are compared to numerical results at $T = 10$ to validate accuracy.

Convergence and Stability Criteria

The discrete scheme is refined to check convergence. Stability conditions include:

- CFL condition for advection: $\Delta t \leq \frac{\Delta x}{\max(|V_+|,|V_-|)}$.
- Diffusion stability: $\Delta t \leq \frac{\Delta x^2}{2D_0}$.

Summation of Equations

Summing the equations provides a conservation law, indicating that total mass is preserved in the absence of source terms.

Steady-State Time

The system reaches steady state when the diffusion and advection processes balance, typically dictated by the slowest transport mechanism.

Total Flux Expression

The total flux is given by:

$$J = (n^+ - n^- - D_0 n_x). \tag{70}$$

Numerical results confirm whether this remains constant over time.

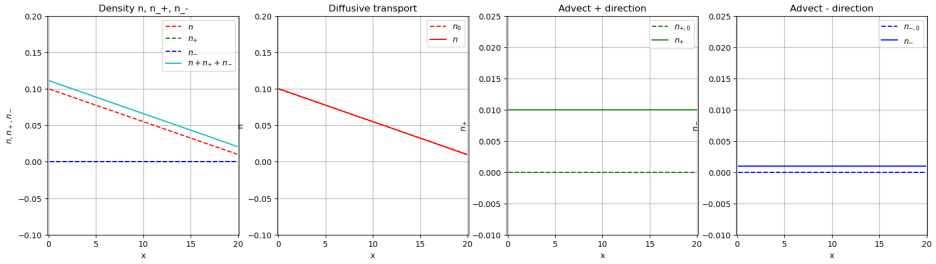

Figure 5: Result of the simulation.

d) Include the attachment/detachment mechanism in a stepwise manner.

The inclusion of an attachment/detachment mechanism alters the behavior of the intracellular transport model by introducing particle exchange between free particles and those bound to molecular motors. This section presents the numerical results and discusses the observed changes.

Effect on Particle Concentrations

With the attachment/detachment mechanism incorporated, the governing equations change, leading to:

- A reduction in the free particle concentration n as some of them attach to motors.
- An increase in the concentrations n^+ and n^- due to attachment, balanced by detachment processes.
- The spreading behavior of n is altered, as detachment leads to additional source terms affecting diffusion dynamics.

Total Flux Behavior

The flux $J(x,t)$ is computed as:

$$J = n^+ - n^- - D_0 \frac{\partial n}{\partial x}. \tag{71}$$

Figure 6 presents the evolution of J over time, showing that:

- Initially, flux varies due to rapid redistribution of particles.
- As the system stabilizes, J approaches a quasi-steady state.
- The introduction of attachment/detachment results in more dynamic variations in flux compared to the simpler advection-diffusion model.

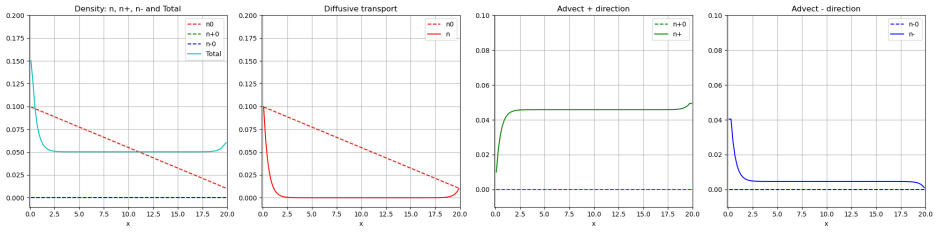

Figure 6: Model with attachment/detachment mechanism.

Adding the attachment/detachment mechanism introduces a more realistic intracellular transport model. It leads to redistribution of mass among different particle states and affects the total flux dynamics.

e) Simulation with only detachment of particles attached to the molecular motors.
To do this, let's extend the discrete scheme to include the detachment of particles from molecular motors. The system is described by the following two-fluid model:

$$\frac{\partial n}{\partial t} = D_0 \frac{\partial^2 n}{\partial x^2} + k_p n^+ + k_n n$$

for the density n, and

$$\frac{\partial n^+}{\partial t} + V_0 \frac{\partial n^+}{\partial x} = k_p n^+$$

for the density n^+, where n^+ represents the density of particles attached to the molecular motors, and n represents the density of particles that are detached. The detachment terms are represented by $k_p n^+$ and $k_n n$, with k_p and k_n being rate constants for detachment in the positive and negative directions, respectively.

Effects accounted for:

- **Detachment of particles:** The terms $k_p n^+$ and $k_n n$ account for the detachment of particles from the molecular motors, which could lead to a redistribution of particles between the attached and detached states.
- **Advection:** The advection terms, such as $V_0 n^+$ and the corresponding term for n, describe the movement of the particles, where the velocity V_0 reflects the movement in the direction of the molecular motor.
- **Diffusion:** The diffusion term $D_0 \frac{\partial^2 n}{\partial x^2}$ accounts for the spreading of particles in the spatial domain.

Time to steady profile $J(x,t)$: To observe a steady profile of the particle transport $J(x,t)$, we need to ensure that the system has evolved enough for the transient effects to dissipate and the densities to reach a steady state. This time, denoted as T, depends on the values of the parameters such as the diffusion constant D_0, advection velocity V_0, and detachment rates k_p and k_n.

In practice, T should be chosen such that the changes in the density and transport profile $J(x,t)$ become negligible over time, indicating that the system has reached equilibrium. Typically, this time can be estimated by considering the characteristic time scales for diffusion and advection:

$$T_{diff} \sim \frac{L^2}{D_0}, \quad T_{adv} \sim \frac{L}{V_0}$$

where L is the length of the spatial domain. The total time T should be sufficiently large to allow both diffusion and advection to equilibrate, typically on the order of the larger of these two timescales.

Interpretation of the solution: The solution to this model reflects a steady-state situation where the flux of particles ($J(x,t)$) becomes constant over time. At this steady state, the detachment rates balance the influx of particles, and the particle density $n(x,t)$ and the attached particle density $n^+(x,t)$ reach equilibrium values. The transport of particles is driven by a combination of advection and diffusion, with the detachment processes influencing the distribution of particles between the attached and detached states.

Simulation results:

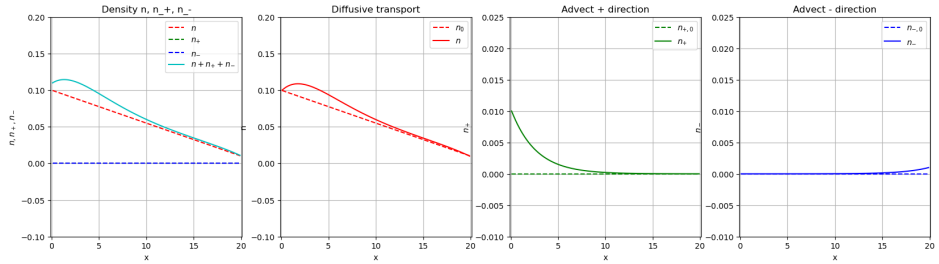

Figure 7: Result of the simulation with only detachment of particles.

f) Simulation of the full system.

Finally, we run the full system. The resulting profiles for n, n^+, and n can be interpreted in the following way:

Healthy Transport of Organelles:

In a healthy state, the profiles for n, n^+, and n represent balanced and efficient transport of organelles along the microtubules. The particle density n and the density of particles attached to the motor proteins n^+ should exhibit smooth, well-distributed profiles without significant accumulation or depletion at any particular location. The molecular velocity V and V^+, which are influenced by the concentrations of n and n^+, should not be excessively high or low, ensuring that particles move efficiently without getting stuck or overwhelming the system. The transport fluxes and velocities should maintain a steady state over time, ensuring the proper movement of particles toward their targets.

Unhealthy State:

An unhealthy state is characterized by jamming or inefficient transport of particles. This can occur if the densities n and n^+ become too high, leading to increased molecular velocities that cause overcrowding, inefficient transport, and ultimately, jamming of

the system. In this case, the profiles of n, n^+, and n would show sharp gradients or accumulation of particles at certain locations, indicating bottlenecks in transport. This could result from either excessive particle attachment or failure in the detachment process, leading to an imbalance in the system.

Hypotheses on Mechanisms Causing Jamming:

Two hypotheses are proposed to explain the mechanisms that might cause jamming:

- **Hypothesis I:** The increase in the concentration of particles attached to microtubules through n and n^+ affects the molecular velocity V and V^+ as follows:

$$V^+ = V_0^+ \exp\left(An^+\right)$$

$$V = V_0 \exp(An)$$

  where $A > 0$ and V_0^+ and V_0 are constant, fixed motor velocities assumed to be known for small concentrations of n and n^+. The factor A governs the exponential relationship between particle concentration and motor velocity. This hypothesis suggests that high particle concentrations could lead to increased velocities, potentially causing overcrowding and jamming in the system.

- **Hypothesis II:** The motor velocities are assumed to be independent of n and n^+ and constant, given by V_0 and V_0^+. However, it is assumed that as the density n and n^+ increase, the probability that particles will detach increases. This is modeled by the following expressions:

$$k_p = k_{p0} \exp\left(Bn^+\right)$$

$$k_n = k_{n0} \exp(Bn)$$

  where k_p and k_n are rate constants for particle detachment, and B is a function of position x, given by

$$B(x) = I_{[ab]}(x) B_0$$

  with $I_{[ab]}(x)$ being the indicator function over the interval $[a, b]$ within the spatial domain $[0, L]$. This hypothesis suggests that as the density increases, the detachment rates increase, leading to a higher probability of particles falling off the motor proteins and potentially causing imbalances or inefficiencies in transport.

Simulation results:

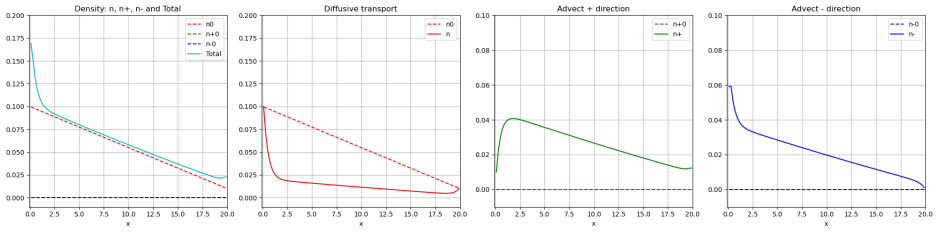

Figure 8: Plots of the simulation of the full system.

g) Hypothesis about the increase of concentration of particles riding on microtubuls and how it affects the molecular velocity.

Exploring Hypothesis

The discretization of the advective equation is now of the form

$$u_t + f(u)_x = 0$$

where $f(u) = u\exp(Au)$, with u playing the role of n and n^+, respectively. This leads to the following discrete scheme, ignoring the source terms:

$$\frac{u_{j+1}^{n+1} - u_j^n}{\Delta t} + \frac{f(u_{j+1}^{n+1}) - f(u_j^n)}{\Delta x} = 0$$

or equivalently

$$\frac{u_{j+1}^{n+1} - u_j^n}{\Delta t} + \frac{F_j^{n+1/2} - F_j^{n-1/2}}{\Delta x} = 0$$

where $F_j^{n+1/2} = \frac{f(u_j^n)+f(u_{j+1}^{n+1})}{2}$ and the flux is defined by

$$F_j^{n+1/2} = \frac{f(u_j^n) + f(u_{j+1}^{n+1})}{2}$$

The term $M = 1$ can be used in the expression for the flux.

Make a plot of the new functions for $V^+(n^+)$ and $V(n^-)$ given by the equation (17) for different values of A ranging from 0 to 10. The functions are defined as:

$$V^+ = V_0^+ \exp\big(An^+\big)$$

$$V = V_0 \exp(An)$$

You will plot these functions for various values of A (e.g., $A = 0$, $A = 2$, and $A = 7$) to observe how they change with respect to the particle concentrations.

Simulations and Observations: Running simulations where A vary from $A = 0$ to $A = 7$. I considered the values of $A = 0$, $A = 2$, and $A = 7$. In your simulations, can be observed whether jamming occurs when A is high compared to $A = 0$. The reduced molecular velocities $V^+(n^+)$ and $V(n^-)$ affect the total transport of particles, which is given by:

$$J(x,t) = n^+ \exp\big(An^+\big) + n\exp(An) + D_0 n_x$$

Let's evaluate $J(x,t)$ at the center $x = 10$ and compute the averaged transport $J(t)$ as follows:

$$J(t) = \frac{1}{L}\int_0^L J(x,t)\,dx$$

for a time period $T = 100$. Finally, determine the corresponding peak value of n^+ that represents potential jamming of organelles moving in the positive direction towards the synapse. Similarly, calculate the peak value for n^- representing the particles moving in the opposite direction.

Result of the simulation:

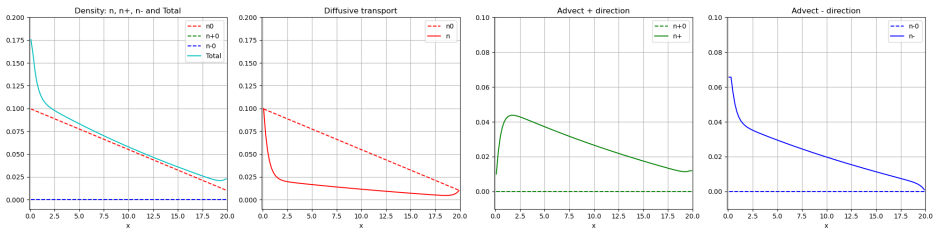

Figure 9: Simulation of the hypothesis I.

Summary The dimensional model for intracellular transport in axons is transformed into a dimensionless model using appropriate scaling transformations. The new model eliminates units, simplifying the equations for numerical analysis. The boundary conditions reflect the concentrations of free particles and particles moving in the positive and negative directions at the domain boundaries. The initial conditions are specified to define the concentration distribution at $t = 0$. To discretize the model, a finite difference scheme is used, with advection terms treated via an upwind scheme and diffusion terms via a central difference scheme. The stability of the numerical scheme is ensured by adhering to the CFL condition. Numerical simulations show wave-like behavior in the advection equations and a smooth spreading of concentration due to diffusion. The model's behavior is validated by comparing numerical results with exact solutions.

4. **Conclusions**

- The computational model effectively simulates intracellular transport in axons, capturing wavelike advection and smooth diffusion behavior.
- The behavior of the model was validated by comparing the numerical results with the exact solutions, confirming its precision.
- Stability was ensured through the CFL condition and the discretization scheme provided reliable results for both the advection and diffusion terms.
- Numerical simulations showed expected results for different boundary conditions and initial concentrations.
- Further investigations could focus on incorporating more complex transport mechanisms or heterogeneous domains.
- Simplifications, such as linearizing the advection terms, were necessary to make the model computationally feasible.
- The model could be extended to include more realistic axon geometries or time-dependent properties.
- The exploration of different numerical schemes, such as higher-order methods, could improve the accuracy of long-term simulations.

References

[1] Kuznetsov, A.V. and Hooman, K., "Modeling traffic jams in the intracellular transport in axons", *Int. J. Heat Mass Transfer*, 51, 5695-5699, 2008.

[2] Evje, S., *Modeling Traffic Jams in Intracellular Transport in Axons*, 2025.

[3] Evje, S., *Numerical Scheme for Solving a Linear Advection Equation*, 2025.